Proceedings of 15th IOE Graduate Conference
Peer Reviewed
Year: 2024 Month: May Volume: 15
ISSN: 2350-8914 (Online), 2350-8906 (Print)

Analysis of Effects of Loading Conditions on Condition Monitoring of Induction Machines

Chandan Pokhrel [a], Nava Raj Karki [b], Basanta Kumar Gautam [c]

[a, b, c] *Department of Electrical Engineering, Pulchowk Campus, Institute of Engineering, Tribhuvan University, Nepal*
[a] 078mspse006.chandan@pcampus.edu.np

Abstract
Induction machines are used in a different range of applications because of their low cost, robustness, and high efficiency. All machines, no matter how robust they are or how well they are designed, are prone to faults during their operation. Broken rotor bar faults is one of such faults and can cause a number of unwanted effects in induction motors. Condition monitoring is required to detect those faults in its inception stage to minimize the down time, economic losses and safety risks. The broken rotor fault produces the sidebands components around the fundamental frequency. By analysing the frequency spectrum of the motor input current for the sidebands, the broken rotor fault can be detected. In this paper, Discrete Fourier Transform is used to analyze the input current of the squirrel cage induction motor to study the effects of the variation of the changing load level on the sidebands to differentiate between healthy and faulty motor states.

Keywords
Induction Motor, Condition Monitoring, Fourier Transform, Broken Rotor Bars

1. Introduction

1.1 Background

Electrical machines are used in a vast number of applications, including but not limited to those in home appliances, electric vehicles, manufacturing process, and power generation. These electrical machines come in various sizes, ranging from a fraction of kilowatts used in household applications, to hundreds of megawatts used in electricity generation. Among them the induction machine consumes around 85% of power in the industrial applications [1]. Induction machine finds its various applications because of its low cost, high efficiency, and robustness [2]. But, no matter how robust a machine is, it is prone to failure at some point of its lifetime. Some of the induction machine faults are broken rotor faults, eccentricity faults, bearing faults, single phasing, and stator winding short circuits. Although broken rotor bars represent around 10% of motor failure, depending on the failure level, they may produce total motor loss [1]. Condition monitoring is the detection of the faults in its inception states before leading to catastrophic failure in order to minimize the down time, economic losses, safety risks, and total motor loss.

1.2 Causes of broken rotor bar

Broken rotor bar faults occur when one or more of the bars that make up the rotor breaks. The failure is caused by the combination of one or more of the following [3, 4].

- Overheating of the rotor cage due to direct on-line starting or overloading.
- Mechanical stress due to pulsating loads, unbalanced load, bearing failures, excessive vibrations, and voltage fluctuations.
- Magnetic stress due to unbalanced electromagnetic forces.
- Contamination and corrosion due to chemical or moisture exposure.
- Manufacturing defects.

1.3 Effects of broken rotor bar on machine operation

A broken rotor bar carries little to no current depending on the degree of the fault. This causes rotor current to be unbalanced [6]. A motor can operate in this asymmetrical condition but results in unbalanced air gap flux, increased losses, increased torque oscillations and decrease in average torque [7]. Due to increase in losses and decrease in average torque, the motor slip increases at constant load as the severity of the fault increases. As the broken bar is unable to conduct the current originally flowing through it, the currents in the neighboring bar increases. Figure 1 [5] shows the current density distribution of squirrel cage motor under healthy and faulty conditions. It shows that the current density increases in the bar close to the broken bar and the effect is more pronounced as the severity of the fault increases. This increase in current leads to an increase in temperature of the rotor and increase losses since the heat loss is directly proportional to the square of the current flowing through it. This increase in heat and temperature of the rotor bar causes the rotor to expand and thus increases the tension in the bar. Increased temperature,

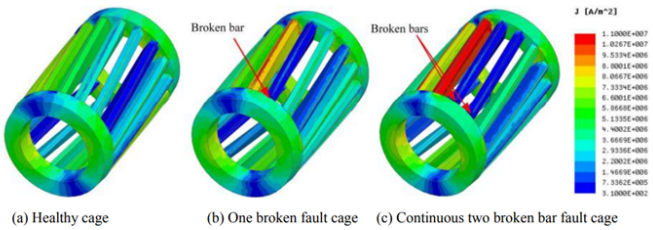

Figure 1: The current density distribution of squirrel cage machine at healthy and faulty condition [5]

electrical stress, and mechanical stress will deform the rotor over time and increase the failure probability of the adjacent rotor bar. This can then escalate to other rotor bars.

In the motor with the high rotor speed, the broken rotor bar may experience sufficient centrifugal forces and can bend toward the stator. This rotor bar may then come in contact with the stator winding leading to the motor failure [8].

2. Methodology

This section describes the experimental method, and the tools and technique used to detect the broken rotor bar faults in the induction machine. The method used here is an non-invasive condition monitoring technique and does not require the direct access to the motor for its implementation. This method requires the stator current of the motor which is easily accessible since, it is utilized for the protection of motor from over currents.

2.1 Stator Current Sidebands

The stator input current contains the information about the machine health. The operation of the induction machine with broken rotor bar induces the line currents at the frequencies given by [9, 10]

$$\mathbf{f_{brb}} = \mathbf{f_s}(\mathbf{m} \pm \mathbf{2ks})$$

where,
$\mathbf{m} = 1, 3, 5, \ldots$
$k \in \mathbb{N}^+$
$\mathbf{f_s}$ is the fundamental component of the stator current
$\mathbf{s}$ is the motor slip

which are known as the side band components. An increment in the magnitude of theses characteristics frequency in the stator current indicates a rotor bar fault. Therefore, the study of these frequencies is a viable option to differentiate motor states.

The magnitude of the components in $\mathbf{f_{brb}}$ decreases rapidly with increase in $\mathbf{k}$ and $\mathbf{m}$. This is shown in Figure 2 [11] and as such they are often limited to 3.

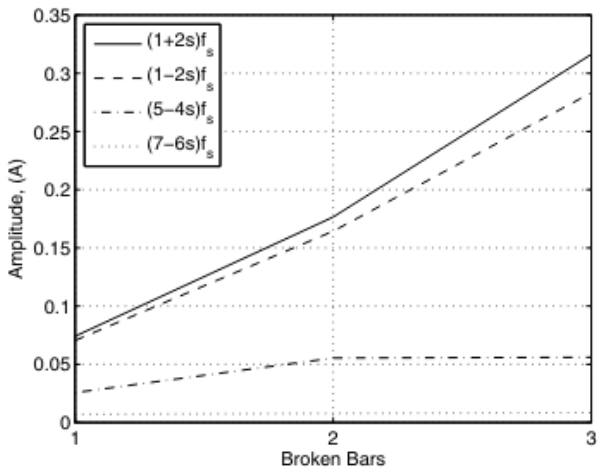

Figure 2: Variation of the magnitue of sidebands

In this paper, the sidebands corresponding to $\mathbf{k} = 1$ and $\mathbf{m} = 1$ is studied. The sideband $\mathbf{f_s(1-2s)}$ is termed as Left Side Band (LSB) and $\mathbf{f_s(1+2s)}$ is termed as Right Side Band (RSB).

2.2 Experimental Setup

The stator input currents for both healthy and faulty states was obtained from the experimental setup at Aalto University, Finland and Tallin University of Technology, Estonia.The machine specification is shown in Table 1.

Parameters	Units	Value
Number of poles		4
Number of Phases		3
Connection		Δ
Voltage	V	400
Current	A	15.3
Power	kW	7.5
Speed	rpm	1460
Power factor		0.79

Table 1: Machine Parameters

The experimental setup is shown in Figure 3. The experiment consists of two identical motors connected back-to-back through their shaft and placed on the same mechanical base. The first healthy motor is use to load the second motor which had 0 to 3 Broken rotor bars. Broken rotor bars were implemented by drilling a hole through the rotor.

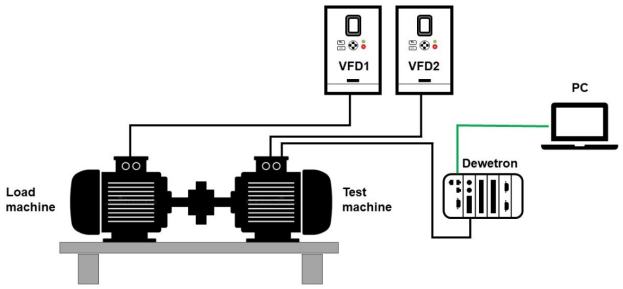

Figure 3: Block diagram of the setup

First, the test machine's phase current was recorded for 20 seconds after steady state under healthy conditions (i.e., at 0 broken rotor bar fault) at different load levels of 0, 25, 50, 75, and 100 percent of the rated nominal load at the sampling rate of 20kHz. Next the rotor bar was broken by drilling a hole in the rotor slot. The bars were broken sequentially, and the current signal recordings were obtained for 1, 2, and 3 broken rotor state. The recordings were stored in a .mat files. Figure 4 - Figure 6 shows the sample measured current signal of the test machine at different states. From, Figure 4 - Figure 6, it can be seen that the machine states are difficult to differentiate based only on time domain signal. Hence, the Discrete Fourier Transform (DFT) was applied to the measured current signals to obtain the frequency spectrum.

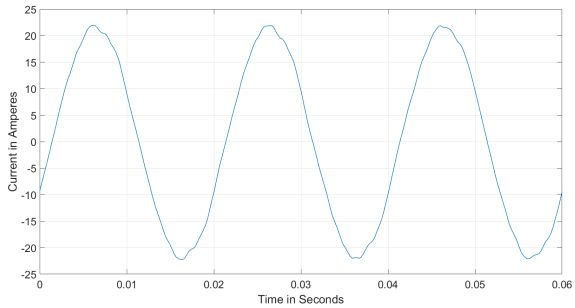

Figure 4: Current Profile from Test Machine with 0 Broken Rotor Bar at 100% Load

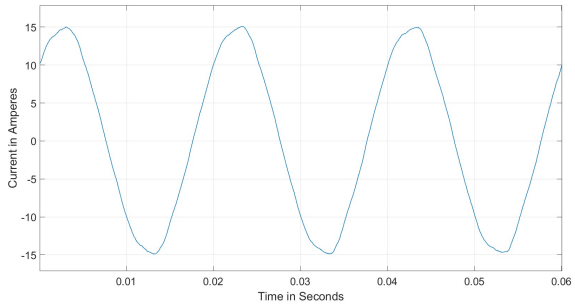

Figure 5: Current Profile from Test Machine with 3 Broken Rotor Bar at 50% Load

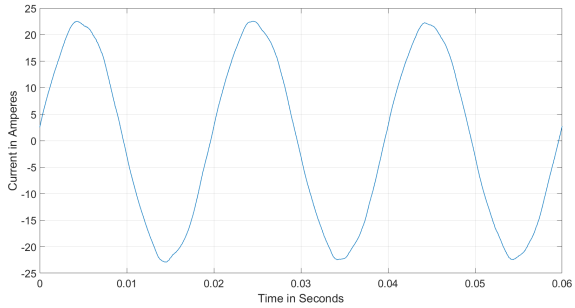

Figure 6: Current Profile from Test Machine with 3 Broken Rotor Bar at 100% Load

2.3 Discrete Fourier Transform

Let x_n be a sequence of the N measured values.

$$x_n = x_0, x_1, x_2, ..., x_{N-1}$$

Then the DFT of the sequence x_n is defined as

$$X_K = \frac{1}{N} \sum_{n=0}^{N-1} e^{-\frac{j2\pi Kn}{N}}$$

where $X_K = X_0, X_1, ..., X_{N-1}$ is the DFT of the sequence x_n and j is the imaginary unit.

3. Results and Discussion

Figure 7 - 11 shows the DFT of the measured current signal at various load levels and various healthy and faulty states. The states are labeled as below:

- Healthy: Motor with no broken rotor bar faults
- 1BRB: Motor with one broken rotor bar
- 2BRB: Motor with two consecutive broken rotor bars
- 3BRB: Motor with three consecutive broken rotor bars.

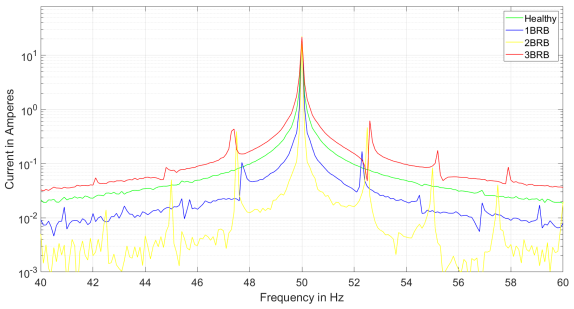

Figure 7: Frequency Spectra of Motors with Healthy and Broken Rotor Bars at 100% of rated load

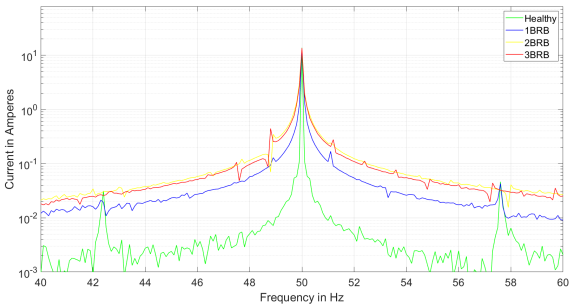

Figure 8: Frequency Spectra of Motors with Healthy and Broken Rotor Bars at 75% of rated load

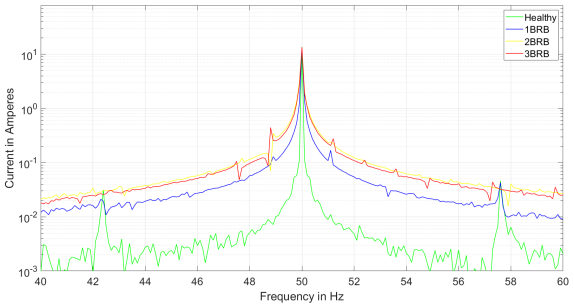

Figure 9: Frequency Spectra of Motors with Healthy and Broken Rotor Bars at 50% of rated load

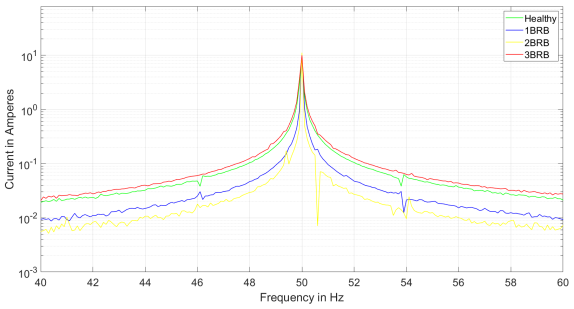

Figure 10: Frequency Spectra of Motors with Healthy and Broken Rotor Bars at 25% of rated load

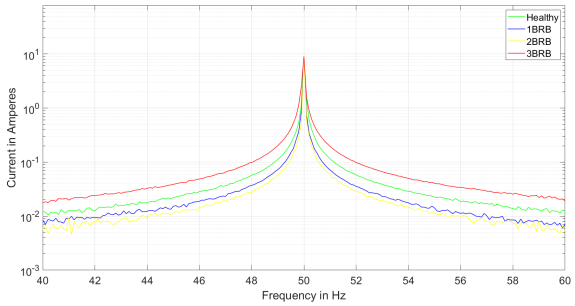

Figure 11: Frequency Spectra of Motors with Healthy and Broken Rotor Bars at 0% of rated load

From the frequency spectra shown in Figure 7-11, it can be easily seen that the side band arises around the fundamental component. The magnitude of the bands at either side of the fundamental frequency was found to increase with the increase in the severity of the fault. Also, the side bands were found to shift away from the fundamental component with the increase in severity of the fault. The sidebands were difficult to observe in low and no load condition on both healthy and faulty states.

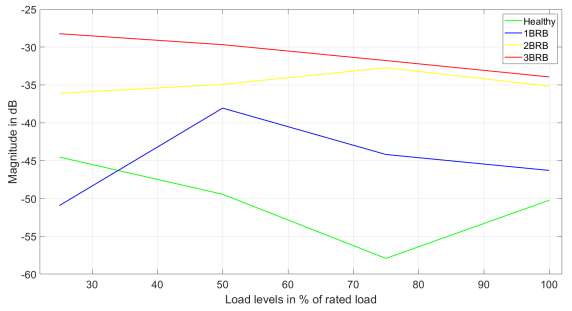

Figure 12: Magnitude of Left Side Band at various load levels

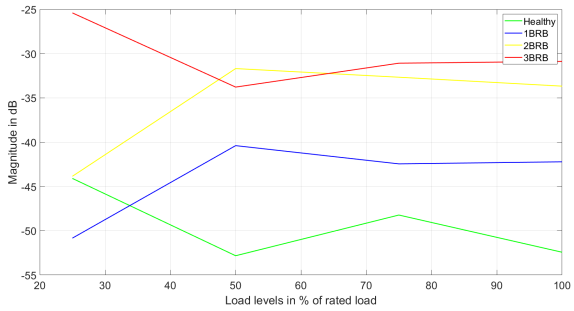

Figure 13: Magnitude of Right Side Band at various load levels

Further, Figure 12 and Figure 13 show the variation of the magnitude of the side bands around the fundamental frequency which can be used to detect the broken rotor bar faults in induction machine. The reason for the difficulty to detect the sidebands at low and no load conditions is due to the fact that the slip **s** decreases with the decrease in loading of the motor and the side band frequencies given by $\mathbf{f_s(1-2s)}$ and $\mathbf{f_s(1+2s)}$ shifts close to the supply frequency $\mathbf{f_s}$. Also, the decrease in the magnitude of the input current at lower loading causes the sidebands to decrease in magnitudes, further making it difficult for their detection.

4. Conclusion

In this paper, frequency analysis was presented as a way to detect the broken rotor faults in induction motor. Section 3 showed that by observing the side bands around the fundamental frequency, the broken rotor faults in induction motor could be detected. An ANN model could be trained to detect the faults in the motors efficiently. Further investigation is needed to detect the fault during the lower loading of the machine.

Acknowledgments

This work was supported by the Department of Electrical Engineering and Automation, Aalto University, Finland under the project Capacity Enhancement in Electrical Equipment Condition Monitoring and Fault Diagnostics (CEEECoM).

References

[1] J. Rangel-Magdaleno, J. Ramirez-Cortes, and H. Peregrina-Barreto, "Broken bars detection on induction motor using mcsa and mathematical morphology: An experimental study," in *2013 IEEE International Instrumentation and Measurement Technology Conference (I2MTC)*, pp. 825–829, 2013.

[2] C. Terron-Santiago, J. Martinez-Roman, R. Puche-Panadero, and A. Sapena-Bano, "A review of techniques used for induction machine fault modelling," *Sensors (Basel, Switzerland)*, 2021.

[3] S. Bindu and V. V. Thomas, "Diagnoses of internal faults of three phase squirrel cage induction motor — a review," in *2014 International Conference on Advances in Energy Conversion Technologies (ICAECT)*, pp. 48–54, 2014.

[4] S. Nandi, R. Bharadwaj, H. Toliyat, and A. Parlos, "Study of three phase induction motors with incipient rotor cage faults under different supply conditions," in *Conference Record of the 1999 IEEE Industry Applications Conference. Thirty-Forth IAS Annual Meeting (Cat. No.99CH36370)*, vol. 3, pp. 1922–1928 vol.3, 1999.

[5] Y. Xie, Z. Wang, X. Shan, and Y. Li, "Investigation of rotor thermal stress in squirrel cage induction motor with broken bar faults," *COMPEL - The international journal for computation and mathematics in electrical and electronic engineering*, 2015.

[6] A. Guedidi, W. Laala, A. Guettaf, and S. E. Zouzou, "Diagnosis and classification of broken bars fault using dwt and artificial neural network without slip estimation," in *2020 XI International Conference on Electrical Power Drive Systems (ICEPDS)*, pp. 1–7, 2020.

[7] I. Ouachtouk, S. El Hani, S. Guedira, K. Dahi, and H. Mediouni, "Broken rotor bar fault detection based on stator current envelopes analysis in squirrel cage induction machine," in *2017 IEEE International Electric Machines and Drives Conference (IEMDC)*, pp. 1–6, 2017.

[8] M. R. Hans and P. D. Mane, "Detection of broken rotor bar along with thermal overload protection," in *2017 2nd International Conference on Communication and Electronics Systems (ICCES)*, pp. 414–419, 2017.

[9] I. Ouachtouk, S. El Hani, S. Guedira, and K. Dahi, "Detection and classification of broken rotor bars faults in induction machine using k-means classifier," in *2016*

International Conference on Electrical and Information Technologies (ICEIT), pp. 180–185, 2016.

[10] B. Amel, Y. Laatra, S. Sami, and D. Nourreddine, "Classification and diagnosis of broken rotor bar faults in induction motor using spectral analysis and svm," in *2013 Eighth International Conference and Exhibition on Ecological Vehicles and Renewable Energies (EVER)*, pp. 1–5, 2013.

[11] G. R. Bossio, C. H. De Angelo, C. M. Pezzani, J. M. Bossio, and G. O. Garcia, "Evaluation of harmonic current sidebands for broken bar diagnosis in induction motors," in *2009 IEEE International Symposium on Diagnostics for Electric Machines, Power Electronics and Drives*, pp. 1–6, 2009.